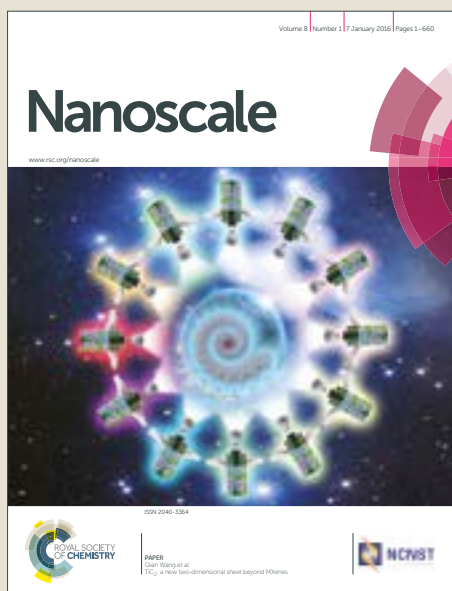


# Nanoscale

Accepted Manuscript



This article can be cited before page numbers have been issued, to do this please use: A. Aziz, T. Zhang, F. Daneshvar, Y. Lin, H. Sue and M. Welland, *Nanoscale*, 2017, DOI: 10.1039/C7NR02478A.



This is an Accepted Manuscript, which has been through the Royal Society of Chemistry peer review process and has been accepted for publication.

Accepted Manuscripts are published online shortly after acceptance, before technical editing, formatting and proof reading. Using this free service, authors can make their results available to the community, in citable form, before we publish the edited article. We will replace this Accepted Manuscript with the edited and formatted Advance Article as soon as it is available.

You can find more information about Accepted Manuscripts in the [author guidelines](#).

Please note that technical editing may introduce minor changes to the text and/or graphics, which may alter content. The journal's standard [Terms & Conditions](#) and the ethical guidelines, outlined in our [author and reviewer resource centre](#), still apply. In no event shall the Royal Society of Chemistry be held responsible for any errors or omissions in this Accepted Manuscript or any consequences arising from the use of any information it contains.



## Nanoscale

## ARTICLE

## 1D Copper nanowires for flexible printable electronics and high ampacity wires

A. Aziz<sup>a†‡</sup>, T. Zhang<sup>b ‡</sup>, Y. H. Lin<sup>b</sup>, F. Daneshvar<sup>b</sup>, H.J. Sue<sup>b†</sup>, and M. E. Welland<sup>a</sup>

Received 00th January 20xx,  
Accepted 00th January 20xx

DOI: 10.1039/x0xx00000x

www.rsc.org/

This paper addresses the synthesis and a detailed electrical analysis of individual copper nanowires (CuNWs). One dimensional CuNWs are chemically grown using Bromide ions (Br<sup>-</sup>) as a co-capping agent. By partially replacing alkyl amines with Br<sup>-</sup>, the isotropic growth on Cu seeds was suppressed during the synthesis. To study the electrical properties of individual CuNWs, a fabrication method is developed which does not require any e-beam lithography process. Chemically grown CuNWs have an ampacity of about 30 million amps per cm<sup>2</sup>, which is more than one order of magnitude larger than the bulk Cu. These good qualities easy to synthesize CuNWs are an excellent candidate for creating high ampacity wires and flexible printable electronics.

### Introduction

One dimensional (1D) conducting wires are important building blocks of the nanotechnology devices. Preparation of 1D nanowires can broadly be divided in to two types. The first type needs a substrate or a template to be grown or supported. For example, nanowires or carbon nanotubes growth on a substrate<sup>1,2</sup>, growth of nanowires using alumina templates<sup>3</sup> or the fabrication of nanowires using any lithography process comes into this category. The second type is the one where nanowires can be grown without a substrate or a template. For example, nanowires grown in a chemical using hydrothermal process<sup>4</sup>. Chemical growth of nanowires is particularly useful for creating cost effective nanowires in a large quantity. The main advantage being that the chemical growth methods can be scaled up to an industrial level.

Due to the recent development in the flexible, stretchable and wearable electronics, and display technology, highly conductive printable transparent conductors are highly desirable. Low dimensional conducting materials are particularly suitable for integrating with flexible substrates. If the electrical conductivity of the nanowires is high, a low density network of nanowires can be used as a transparent conductor. For example, Ag nanowires have been used for creating flexible, transparent and stretchable electrode<sup>5,6,7</sup>. Cu<sup>4</sup>, Au<sup>8</sup> and Ag<sup>9</sup> are some of the conducting metals which can

be chemically grown into long nanowires without any substrate or template. In particular, Cu has one of the highest electrical conductivity (~6x10<sup>5</sup> S/cm) among materials. It is also much cheaper than Ag and Au, and abundant in nature. Therefore, Cu is a material of choice for applications which require high electrical conductivity and flexibility. Copper nanowires (CuNWs) also have a high electrical conductivity as compared to the metal oxides like ITO (Indium Tin Oxide)<sup>10</sup> or carbon based materials<sup>11</sup>. In this paper we study the chemical growth of low dimensional Cu nanostructures using hydrothermal process and co-capping agent, and investigate the electrical properties and the failure mechanism of the individual nanowires.

CuNWs can be chemically grown to hundreds of microns in length. These nanowires can make a network of highly flexible conducting wires. One drawback is that the CuNWs surface can get oxidized in air, either a capping layer like polyimide or PDMS can be used to protect it from oxidation or CuNWs can be covered with a graphene layer<sup>12</sup>. For large area applications, methods like photonic welding or laser induced photochemical reduction of CuxO NW to CuNW can also be used for improving conductive links between CuNWs<sup>13,14</sup>. Electrical properties of CuNWs are commonly measured using sheet resistance<sup>15</sup>, where current pass through a percolation path. It provides some electrical conductivity information which is averaged over a large but unknown number of nanowires. High contact resistance, which is due to a large number of wires junctions, dominates the resistance and therefore it is hard to measure the true electrical conductivity and the ampacity of the CuNWs. To understand the quality of nanowires, individual CuNWs must be analyzed. Xu *et al.* studied the transport properties of a single Cu nanowire but they could not determine the ampacity of the CuNWs because their Pt contacts had lower ampacity

<sup>a</sup> Nanoscience Centre, Department of Engineering, University of Cambridge, CB3 0FF, UK.

<sup>b</sup> Polymer Technology Centre, Department of Materials Science and Engineering, Texas A&M University, College Station, TX 77843, USA.

† Corresponding authors: A. Aziz: aa267@cam.ac.uk, H.J. Sue: hjsue@tamu.edu  
Electronic Supplementary Information (ESI) available: [Additional SEM images of Cu nanocrystals, contact resistance and Pt conductivity are provided in the supplementary information]. See DOI: 10.1039/x0xx00000x

than CuNWs.<sup>16</sup> In this work, we have developed a simple method, which does not require an e-beam lithography process, to fabricate transport devices using a single CuNW and these devices do not suffer from the problem faced by Xu *et al.* Electrical properties, which include electrical conductivity, current carrying capacity, and failure mechanism, of the chemically synthesized CuNWs were carefully investigated.

## Synthesis of Cu nanowires (CuNWs)

Synthesis of CuNWs through a hydrothermal method has been considered as a promising strategy for large-scale production of nanomaterials.<sup>17</sup> In a typical synthesis system, as illustrated in Figure 1(a), copper ions, Cu (I) or Cu (II), are reduced to Cu (0) seeds, and then 1D growth on these nanocrystal seeds in aqueous or organic solutions leads to the formation of CuNWs.<sup>18,19,20</sup> Among these systems, alkyl amines were mostly used, because they not only served as a capping agent but also complexed with other reactant to promote the seed formation and the chemical reduction process.<sup>21,22</sup> This multi-functional role makes alkyl amines irreplaceable in Cu nanowire synthesis. However, it is a challenge to use alkyl amines as a sole capping agent to produce clean CuNWs because a relatively large fraction of other shapes for Cu nanocrystals, such as particles, cubes, is also produced, as seen in Figure 2. The capping insufficiency is the reason for the isotropic crystal growth in these systems.

In order to better control the growth kinetics to suppress the isotropic crystal growth, one solution is to incorporate a co-

capping agent to modify the capping efficiency. Bromide ions ( $\text{Br}^-$ ) have been widely used to initiate the anisotropic growth on Au, Ag or Pt nanocrystals.<sup>23</sup> Similar to alkyl amines,  $\text{Br}^-$  preferentially adsorbs onto {100} facet on metal nanocrystals to restrict the growth direction.<sup>23</sup> The ionic species with a relatively small size like  $\text{Br}^-$  can have a better capping effect than alkyl amines on Cu seeds. In this work, we introduced  $\text{Br}^-$  as a co-capping agent to produce good quality CuNWs.

The precursor solution was obtained by dissolving copper chloride ( $\text{CuCl}_2$ ), glucose, hexadecylamine (HDA) and potassium bromide (KBr) in 60 mL deionized water. A uniform solution in blue color was formed after stirring, indicating the formation of Cu(II)-HDA complexes.<sup>22</sup> The precursor solution was then kept at 110 °C for 16 h without stirring, and the color of the solution was changed from blue to pink and then reddish brown. The color change in the solution indicated that the Cu(II)-HDA complexes have been reduced to Cu seeds, likely through the Maillard's reaction,<sup>21</sup> and then formed CuNWs via 1D nanocrystal growth.

The molar ratio of Cu and capping agent is critical for the control of nanocrystal growth. In the absence of  $\text{Br}^-$ , the capping on Cu nanocrystals was carried out using HDA alone. The preferential adsorption of HDA on {100} facets could suppress the crystal growth on these facets to initiate an anisotropic growth.<sup>18</sup> However, as seen in Figure 2, the sample with a molar ratio of 1:1:3:0 ( $\text{CuCl}_2$ :glucose:HDA:KBr, hereinafter), only produced Cu nanoparticles and nanocubes, indicating an isotropic growth dominated system. The reason is because the concentration of HDA was insufficient to cover

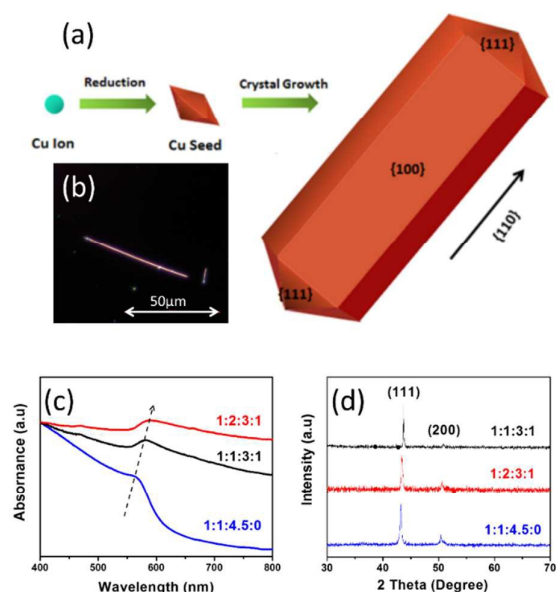


Figure 1. (a) Schematic representation of Cu nanowire synthesis using a hydrothermal method. (b) Dark field optical image. (c) UV-Vis spectra and (d) XRD patterns of the as-synthesized 1D CuNWs.

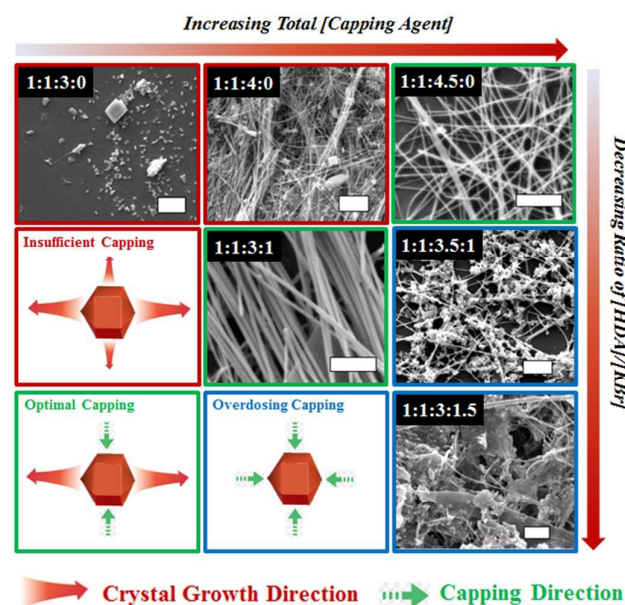


Figure 2. Schematic demonstration of capping effect on the growth of Cu nanocrystals, and the scanning electron micrographs of the Cu nanocrystals synthesized with different molar ratio of  $\text{CuCl}_2$ :glucose:HDA:KBr. Bars = 2  $\mu\text{m}$ .

all newly formed {100} facets on Cu nanocrystals in this

sample. These exposed facets are active for Cu crystal growth, which was demonstrated as *insufficient capping* in Figure 2. With increased concentration of HDA, CuNWs started to form in the system, indicating that anisotropic growth started to dominate the systems. With a molar ratio of 1:1:4.5:0, a large fraction of CuNWs with a diameter of  $72 \pm 13$  nm were obtained.

Incorporation of  $\text{Br}^-$  could modify the capping efficiency on Cu nanocrystals. For example, the nanoparticle formation can be suppressed using  $\text{Br}^-$  as a co-capping agent to partially replace HDA. As shown in Figure 2, the approximate 60% of CuNWs and 40% of nanoparticles were obtained using a molar ratio of 1:1:4:0. With the same molar ratio of Cu and total capping agent, clean CuNWs with only trace amount (about 2-3%) of nanoparticles were synthesized by replacing one quarter of HDA with  $\text{Br}^-$ , i.e., using a molar ratio of 1:1:3:1. It is well known that nanowires grow from multi-twinned seeds.<sup>24</sup> However, multi-twinned seeds are unstable at initial stages if their {100} facets were not well capped. The crystal growth on {100} facets could rapidly develop multi-twinned seeds into single-crystal seeds,<sup>25</sup> which only produce nanoparticles. Compared with more hydrophobic HDA molecule,  $\text{Br}^-$  is a small ionic component which can diffuse faster in an aqueous environment, and easier to be chemisorbed onto nanocrystals, especially onto small nanocrystals ( $< 10$  nm).<sup>25</sup>  $\text{Br}^-$  was also found to facilitate the maturing process for Cu nanocrystals growing in a non-aqueous environment.<sup>26</sup> These features of  $\text{Br}^-$  ensures a well capping on multi-twinned seeds, which is critical to suppress isotropic growth.

The ratio of the HDA and KBr is also important because different HDA:KBr ratio gives different capping efficiency on Cu nanocrystals. On one hand, insufficient  $\text{Br}^-$  cannot provide enough capping protection on Cu seeds, resulting in *insufficient capping*. On the other hand, overdosing  $\text{Br}^-$  can also reduce Cu nanowire formation. If the {100} facets on Cu nanocrystals have been saturated by capping agent, extra  $\text{Br}^-$

can also cap {110} and {111} facets on Cu nanocrystals.<sup>19</sup> As demonstrated in Figure 2, *overdosing capping* can suppress the overall growth of Cu seeds, resulting in formation of small Cu nanocrystals. Sometimes, these small nanocrystals may aggregate to form plate-like structures.<sup>25</sup> This is the reason why using  $\text{Br}^-$  alone cannot produce CuNWs.<sup>19</sup> In this study, an optimal molar ratio to produce CuNWs was found to be 1:1:3:1 (CuCl<sub>2</sub>:glucose:HDA:KBr). The samples with a lower or higher HDA:KBr ratio produced more small nanoparticles. Additional SEM images can be found in the Supplementary Materials.

The CuNWs formation is also affected by the chemical reduction process. The rate of reduction is usually adjustable by varying the concentration of reducing agent, or glucose in this study. More glucose in the system can increase the rate of chemical reduction. In this scenario, faster growth on Cu seeds could lead to more seeds developed from multi-twinned to single-crystal if capping agent failed to stop the crystal growth on {100} facets in time. Figure 3 showed the effect of glucose concentration on CuNWs formation. As expected, more small nanoparticles were observed when the concentration of glucose was doubled in the absence of  $\text{Br}^-$  (1:2:4.5:0). Interestingly, the similar phenomenon was not observed for the samples with  $\text{Br}^-$ . The nanoparticle formation was still suppressed even though we doubled the concentration of glucose, i.e., using a molar ratio of 1:2:3:1. It confirmed that using  $\text{Br}^-$  as a co-capping agent can protect {100} facets on Cu seeds efficiently. As a result, the isotropic growth on Cu nanocrystals was suppressed in the presence of  $\text{Br}^-$ .

The diameter of CuNWs synthesized using  $\text{Br}^-$  was found to be  $176 \pm 29$  nm which is larger than those without using  $\text{Br}^-$  ( $72 \pm 13$  nm). This observation was confirmed using UV-Vis spectroscopy (Figure 1c). Compared with the  $\text{Br}^-$  free sample (1:1:4.5:0), the maximum absorption peaks for the CuNWs synthesized using  $\text{Br}^-$  shifted to higher wavenumbers. Because of the surface plasmon resonance effect,<sup>22</sup> this redshift suggests that the CuNWs in these samples (1:1:3:1 and 1:2:3:1) have a larger average nanowire diameter. One possible reason for the increase in nanowire diameters is that although  $\text{Br}^-$  could protect the Cu seeds in the early stages, the competitive adsorption between  $\text{Br}^-$  and HDA might reduce the packing density for the HDA layers on {100} facets, resulting in the CuNWs with a larger diameter.<sup>26</sup> The other possibility is due to the aforementioned multi-functional role of HDA. HDA is also involved in other process, such as seeding, complexation and reduction.  $\text{Br}^-$ , as far as we know, does not participate in these processes. In addition to capping effect, partially replacing HDA with  $\text{Br}^-$ , therefore, might contribute to other effect on the dislocation-driven growth of Cu seeds, and consequently produces CuNWs with different diameters.<sup>27</sup> The XRD patterns of the as-synthesized CuNWs (Figure 1d) are in consistence with face-centered-cubic Cu without a significant amount of other impurities. The CuNWs synthesized using a molar ratio of 1:1:3:1 were selected for electrical measurement.

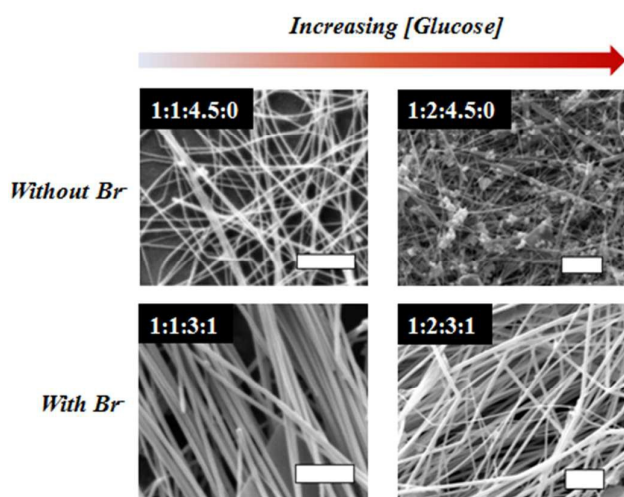


Figure 3. Scanning electron micrographs of the Cu nanowires synthesized with different molar ratio of CuCl<sub>2</sub>: glucose:HDA:KBr. Scale bars = 2  $\mu$ m.

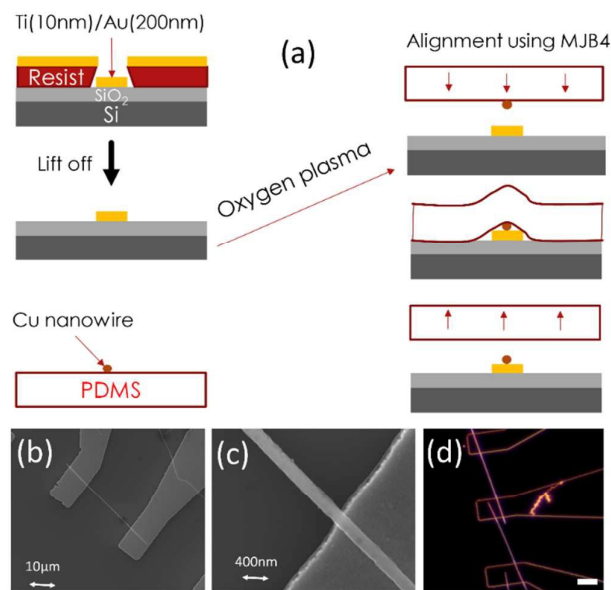


Figure 4. (a) Schematic of the CuNW transfer process from PDMS to the Ti/Au electrode on a Si/SiO<sub>2</sub> wafer. (b-c) SEM images of the CuNW after landing on the Ti/Au electrodes. (d) Dark field optical image of the CuNWs after being landed on the Ti/Au electrodes, scale bar=10 $\mu$ m.

### Fabrication of CuNW transport devices

CuNW transport devices were fabricated using an aligned landing of nanowires onto the Titanium/Gold (Ti/Au) electrodes. The main advantage of this technique is that no complex e-beam lithography is required. Schematic of the process is shown in Figure 4a. First of all, Ti/Au contacts were fabricated using photolithography and the lift off process on a Si/SiO<sub>2</sub> (60nm) wafer. A 10nm Ti layer and then 200nm Au layer was deposited using an e-beam evaporator. A small drop of ethanol solution which contains CuNWs was placed, using a pipette, on a thin (~200 $\mu$ m) Polydimethylsiloxane (PDMS) film and left to dry. CuNWs were 200nm in diameter and about 50 $\mu$ m long. These wires could be seen using an optical microscope. PDMS was then attached to the glass slide. An MJB4 mask aligner was used to align an isolated CuNW on the PDMS layer with the Au electrodes. Immediately before doing the alignment process, silicon chip which had Ti/Au electrodes, was cleaned with an oxygen plasma with RF (Radio Frequency) power 100W and pressure 0.4 mBar for five minutes. Once aligned, silicon chip was slowly raised until it is in contact with the PDMS. Sample was then left to remain in contact for two minutes. PDMS was then slowly removed by lowering the Si wafer down. The transfer was performed using the medium retention 6.5mil PF-40-X4 film from Gel-Pak and no heating was required to transfer the CuNW. Figures 4 (b,c) show the SEM images of the CuNW after being landed on the Ti/Au

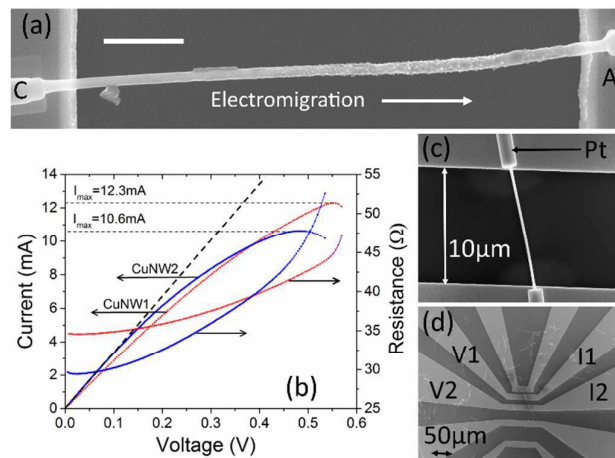


Figure 5. (a) SEM of a CuNW after a large current passes through the wire. Scale bar is 2 $\mu$ m. Anode and cathode are labelled A and C respectively. It shows the effect of electromigration. Electromigration is in the direction of the anode electrode. Length of the wire is about 14 $\mu$ m. (b) IV curves and the corresponding resistance of the nanowires CuNW1 and CuNW2.  $I_{max}$  is the maximum current that passes through the CuNW, after which the current drops and the nanowire becomes an open circuit. The dash line is a straight line drawn along the linear region of the IV curve. (c) SEM image of the devices after Pt deposition using Ga focused ion beam. (d) SEM image of the four-probe device geometry.

electrodes and 4d is the dark field optical image of the CuNWs on the Ti/Au electrodes.

### Electrical measurements:

Four terminal electrical measurements were performed using Keithley 5200 SCS parameter analyzer. The device geometry is shown in Figure 5d. The current was applied between the electrodes I1 and I2 and the voltage drop across the CuNW was measured using the voltage leads V1 and V2. When CuNWs are exposed to air, a thin oxide layer on the Cu wires prevents a good electrical contact between the nanowire and the Au electrodes. To establish a lowest possible contact resistance, a few nanometers of the CuNW was etched using Gallium Focused Ion Beam (Ga-FIB) milling and then about 200nm thick, 1 $\mu$ m wide and 5 $\mu$ m long Platinum (Pt) pads were deposited using a Ga-FIB, as shown in Figure 5c.

Pt contact resistance is measured by drawing the resistance of CuNW1, CuNW2 and CuNW3 as function of their length, as shown in Figure S2. The contact resistance is about 9 $\Omega$ . Table 1 shows the electrical conductivity and the maximum current density or ampacity of the 1D CuNWs measured at room temperature. The electrical conductivity of the nanowires is a little less than Cu. However, the maximum current density of all the CuNWs is close to  $3 \times 10^7$  A/cm<sup>2</sup>, which is more than an order of magnitude larger than the bulk Cu wires.

Table 1. Dimensions, conductivity and the maximum current density of the 1D CuNW.

Sample	Length L(μm)	Diameter d(nm)	Electrical Conductivity σ(S/cm)	Max. Current density J <sub>max</sub> (A/cm <sup>2</sup> )
Cu(Bulk)			5.9×10 <sup>5</sup>	1.0×10 <sup>6</sup>
CuNW 1	28.5	200	3.5×10 <sup>5</sup>	3.9×10 <sup>7</sup>
CuNW 2	20	190	3.4×10 <sup>5</sup>	3.7×10 <sup>7</sup>
CuNW 3	11	190	3.4×10 <sup>5</sup>	3.9×10 <sup>7</sup>

The IV curves and the resistance of the samples CuNW1 and CuNW2 are plotted in Figure 5b. The IV curves are linear up to about 2mA. Nanowires show a linear (Ohmic) behaviour at low bias, as indicated by the projected dashed line. However, as the current is increased further, the resistance of the wire is noticeably increased due to the Joule heating and the IV curve becomes non-linear. After the current reaches the maximum value at  $I_{max}$ , the current drops and CuNW becomes an open circuit. The ampacity of the CuNW is defined as the maximum current density which flows through the wire before it becomes an open circuit. On average, the ampacity of these high aspect ratio CuNWs is  $J = 3.8 \times 10^7$  A/cm<sup>2</sup>, which shows that the chemically grown CuNWs are of good quality and exhibit low density of defects.

### Discussion and analysis:

The electrical conductivity of the CuNW is extracted from the linear regime of the IV curve, and after subtracting the 9Ω Pt contact resistance, the electrical conductivity of the CuNWs is calculated as  $3.4 \times 10^5$  S/cm. It is lower than the electrical conductivity of the bulk Cu, which is typically  $5.95 \times 10^5$  S/cm. Since the width of the wire is greater than the electron mean free path in Cu, which is about 40nm,<sup>28</sup> the grain boundaries

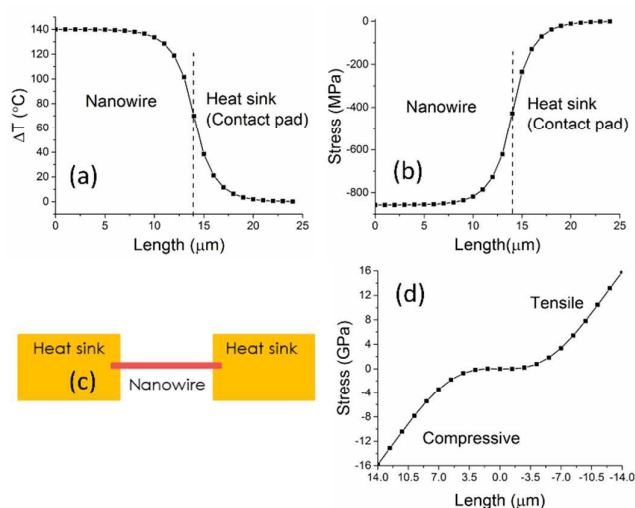


Figure 6. (a) The calculated temperature difference profile of the CuNW at 12.3mA. (b) Thermal stress experience by the CuNW as a function of length. (a) and (b) It shows the profiles from center of the wire to the heat sink. Due to symmetry, profile should be same for the other half of the wire. (c) The cartoon of the device. (d) Compressive and the tensile stress experience by the CuNW due to electromigration.

rather than surface scattering is the dominant mechanism for this lower electrical conductivity. Similar conductivity values ( $1.8 \times 10^5$  S/cm and  $2.8 \times 10^5$  S/cm) are reported for an e-beam evaporated and other hydro thermal CuNW respectively<sup>29, 16</sup>. As compared to chemically grown nanowires, Cu nanowires created using pulsed electrodeposition has lower ampacity of about  $2 \times 10^6$  A/cm<sup>2</sup> where as CuNW grown in vacuum using e-beam evaporation has higher ampacity about  $1 \times 10^8$  A/cm<sup>2</sup>. It should be noted that these CuNWs have much smaller aspect ratio than the ones studied here.<sup>30, 31</sup>

At high current density, the nanowire experiences a thermal as well as an electromigration stresses. The CuNW is connected to the Au electrodes, which function as heat sinks, on both ends. The temperature profile along the nanowire and the heat sink is calculated using heat transfer equation  $\nabla^2 T - m^2 T + Q/k = 0$ <sup>32</sup>. Where  $m = \sqrt{k_{sub}/ktd}$  and  $Q = J^2 \rho$ . The wire is considered as a rectangular wire of width and thickness  $t = 200$ nm and  $2L = 28\mu$ m is the length of the CuNW. The values used for the thermal conductivities of the wire and the substrate are  $k = 385$  W/K/m and  $k_{sub} = 0.55$  W/K/m, respectively. The thickness of the oxide layer underneath the CuNW is  $d = 60$ nm, and  $J = 3.9 \times 10^7$  A/cm<sup>2</sup> is the current density at which the temperature profile is calculated. The temperature profile of the CuNW is shown in Figure 6a. It shows that the temperature is maximum (approximately 140°C) at the centre of the wire, and the temperature gradient is highest near the edges. It also shows that the heat is mainly dissipating from the contact pads. Similar distribution was also observed in silver nanowires.<sup>33</sup> The temperature rise causes the wire to expand with respect to the substrate and therefore creates a thermal stress. Thermal stress is proportional to the thermal coefficient of expansion ( $\beta$ ), the Young's modulus ( $B$ ) and the change in temperature ( $\Delta T$ ) of the nanowire. Figure 6b shows the thermal stress along the wires, calculated using  $Thermal\ stress = -3\beta B \Delta T$ . Where 3 comes from the geometrical factor and negative sign represents the compressive stress, thermal expansion coefficient of Cu relative to SiO<sub>2</sub> used for this calculation is  $\beta = 17 \times 10^{-6}$  °C<sup>-1</sup> and the Young's modulus is  $B = 120$ GPa.

At high current density, electrons wind transfers enough momentum to the Cu atoms such that they are displaced in the direction of the electron flow, leaving behind vacancies. Accumulation of vacancies causes tensile stress; whereas, an accumulation of Cu results in compressive stress. Since vacancies are accumulated near the cathode, tensile stress occurs at the cathode end of the wire; whereas, compressive stress builds up near the anode. Figure 5a shows the CuNW after a current density of  $1 \times 10^7$  A/cm<sup>2</sup> pass through the CuNW. To observe the Cu mass transfer due to an electromigration (EM) effect, voltage was swept at the rate of 0.4mV/s. This image shows that the Cu atoms are accumulated near the anode end of the transport device. EM stress of the CuNW1 sample at 12.3 mA current is calculated using the equation below and plotted in Figure 6d.<sup>34</sup>

$$\sigma = 2GL \left( -\frac{x}{2L} - 4 \sum_{n=0}^{\infty} \left( \frac{1}{\eta^2} e^{-\eta t/\tau} \cos \left( \eta \frac{x+L}{2L} \right) \right) \right)$$

## ARTICLE

## Nanoscale

Where  $G = Eq/\Omega$  is the EM driving force,  $\eta = (2n + 1)\pi$  and  $\tau = 4L^2/\kappa$ ;  $\kappa = DB\Omega/k_B T$  and  $E = J\rho$ .  $D, B, \Omega$  and  $q$  are the effective atomic diffusivity, Young's modulus, atomic volume and the effective atomic charge respectively.  $J$  is the current density and  $\rho$  is the resistivity of the Cu wire.

By comparing between figure 6b and 6d, stress caused by an electromigration is much greater than that due to the thermal stress. The failure location of the wire also gives a good indication of the mechanism involved in breaking the nanowire at high current density. If the failure occurs at the centre of the wire, Joule heating is generally the dominant failure mechanism, as observed by Yeo et al. in silver nanowires.<sup>33</sup> Whereas, if failure occurs at the electrode ends of the wire, tensile or compressive stress due to electromigration causes the wire to fail. We have observed that the CuNWs always fail near the cathode end of the wire, which also shows that tensile stress due to electro migration is the dominant failure mechanism for these CuNWs. Therefore, the ampacity of the CuNW is limited by the electron migration process. The high ampacity in these nanowires, as compared to bulk Cu, is most likely due to the delayed onset of electromigration. Since the presence of voids between metal grains help the onset of the electromigration process. High ampacity indicates that the grains in chemically grown Cu nanowires are well packed and free of voids.

## Conclusion

In summary, Br<sup>-</sup> has been used as a co-capping agent to partially replace alkyl amines to synthesize CuNWs. During the reaction, multi-twinned Cu seeds were efficiently protected by Br<sup>-</sup>, especially at their initial stages, to suppress isotropic growth. With an optimal capping agent ratio of 3:1 (HDA:Br<sup>-</sup>), clean CuNWs with good electrical conductivity and ampacity were synthesized. These CuNWs can be used in various applications that demand high thermal and electrical conductivity and ampacity. Since CuNWs can sustain a high current density, thanks to their good ampacity, only a very low number of chemically grown CuNWs are needed for making transparent and flexible conductors. The CuNWs possess an ampacity one order of magnitude higher than the bulk Cu, and found to be limited by the electromigration process. If electromigration can be suppressed further, the ampacity of the CuNW can be increased more. Despite the fact that these CuNW are grown using a simple solution method, which does not require any vacuum processing, they have a high ampacity and good conductivity. These high quality CuNW can lead to more reliable and robust devices. It is anticipated that high ampacity material systems containing CuNWs can be produced for many important industrial applications, including microelectronic devices, electrical vehicles, flexible, stretchable and transparent devices, composite materials and power grids for energy transmission.

## Acknowledgements

All the authors acknowledge the support of the Lloyd's Register Foundation, London, UK, who has funded this research through their grants to protect life and property by supporting engineering-related education, public engagement and the application of research.

‡These authors contributed equally.

## Notes and references

### Materials used

Copper chloride (CuCl<sub>2</sub>, from Alfa Aesar), glucose (from TCI), hexadecylamine (HDA, from Merck) and potassium bromide (KBr, from J.T. Baker) were used as received.

### Cu nanowires (CuNWs) synthesis

In the precursor solution, typically 0.75 mmol CuCl<sub>2</sub>, 0.75 mmol glucose, and different moles of hexadecylamine (HDA) and KBr were dissolved in 60 mL deionized water. The mixtures were stirred for 7 h, and then kept at 110 °C for 16 h without stirring. The products were collected through centrifugation at 6000 rpm for 10 min, and washed with deionized water, hexane and ethanol 2~3 times each until the supernatant turned clear. The products were stored in ethanol.

### Characterization

The structural properties and the morphologies of the as-synthesized CuNWs were examined using ultraviolet-visible near-infrared spectrophotometer (Shimadzu UV-3600), X-ray powder diffractometer (Bruker D8 focus Bragg Brentano) and scanning electron microscope (FEI Quanta 600 FE-SEM).

### Fabrication of devices

To optimize the transfer of CuNWs on to the gold electrodes different types of PDMS films (PF-30-XT, PF-40-X4, PF-10/17-X4 and PF-60-X8) from Gel-Pak were tested. The best transfer was obtained by using the medium retention 6.5mil PF-40-X4 film. Platinum pads were deposited using FEI FIB200 system at 30KeV and 13pA. It took about 3mins to deposit 200nm thick Pt of dimensions 5μ x 1μm, using dwell time 0.2μs. The electrical conductivity of the FIB deposited Pt was 4.7x10<sup>2</sup> Scm<sup>-1</sup>, see Figure S3.

- (1) Robertson, J. Growth of Nanotubes for Electronics. *Mater. Today* **2007**, *10*, 36–43.
- (2) Park, W. I.; Kim, D. H.; Jung, S. W.; Yi, G. C. Metalorganic Vapor-Phase Epitaxial Growth of Vertically Well-Aligned ZnO Nanorods. *Appl. Phys. Lett.* **2002**, *80*, 4232–4234.
- (3) Xu, X.; Fang, X.; Zeng, H.; Zhai, T.; Bando, Y.; Golberg, D. One-Dimensional Nanostructures in Porous Anodic Alumina Membranes. *Sci. Adv. Mater.* **2010**, *2*, 273–294.
- (4) Ye, S.; Stewart, I. E.; Chen, Z.; Li, B.; Rathmell, A. R.; Wiley, B. J. How Copper Nanowires Grow and How to Control Their Properties. *Acc. Chem. Res.* **2016**, *49*, 442–451.
- (5) Hong, S.; Lee, H.; Lee, J.; Kwon, J.; Han, S.; Suh, Y. D.; Cho, H.; Shin, J.; Yeo, J.; Ko, S. H. Highly Stretchable and Transparent Metal Nanowire Heater for Wearable Electronics Applications. *Adv. Mater.* **2015**, *27*, 4744–4751.

- (6) Lee, J.; An, K.; Won, P.; Ka, Y.; Hwang, H.; Moon, H.; Kwon, Y.; Hong, S.; Kim, C.; Lee, C.; *et al.* A Dual-Scale Metal Nanowire Network Transparent Conductor for Highly Efficient and Flexible Organic Light Emitting Diodes. *Nanoscale* **2017**, *9*, 1978–1985.
- (7) Bari, B.; Lee, J.; Jang, T.; Won, P.; Ko, S. H.; Alamgir, K.; Arshad, M.; Guo, L. J. Simple Hydrothermal Synthesis of Very-Long and Thin Silver Nanowires and Their Application in High Quality Transparent Electrodes. *J. Mater. Chem. A* **2016**, *4*, 11365–11371.
- (8) Kim, F.; Sohn, K.; Wu, J. S.; Huang, J. X. Chemical Synthesis of Gold Nanowires in Acidic Solutions. *J. Am. Chem. Soc.* **2008**, *130*, 14442–.
- (9) Gou, L. F.; Chipara, M.; Zaleski, J. M. Convenient, Rapid Synthesis of Ag Nanowires (Vol 19, Pg 1755, 2007). *Chem. Mater.* **2007**, *19*, 4378.
- (10) Minami, T. Transparent Conducting Oxide Semiconductors for Transparent Electrodes. *Semicond. Sci. Technol.* **2005**, *20*, S35–S44.
- (11) Lipomi, D. J.; Vosgueritchian, M.; Tee, B. C.-K.; Hellstrom, S. L.; Lee, J. a; Fox, C. H.; Bao, Z. Skin-like Pressure and Strain Sensors Based on Transparent Elastic Films of Carbon Nanotubes. *Nat. Nanotechnol.* **2011**, *6*, 788–792.
- (12) Ahn, Y.; Jeong, Y.; Lee, D.; Lee, Y. Copper Nanowire-Graphene Core-Shell Nanostructure for Highly Stable Transparent Conducting Electrodes. *ACS Nano* **2015**, *9*, 3125–3133.
- (13) Mallikarjuna, K.; Hwang, H.-J.; Chung, W.-H.; Kim, H.-S. Photonic Welding of Ultra-Long Copper Nanowire Network for Flexible Transparent Electrodes Using White Flash Light Sintering. *RSC Adv.* **2016**, *6*, 4770–4779.
- (14) Han, S.; Hong, S.; Yeo, J.; Kim, D.; Kang, B.; Yang, M. Y.; Ko, S. H. Nanorecycling: Monolithic Integration of Copper and Copper Oxide Nanowire Network Electrode through Selective Reversible Photothermochemical Reduction. *Adv. Mater.* **2015**, *27*, 6397–6403.
- (15) Guo, H.; Lin, N.; Chen, Y.; Wang, Z.; Xie, Q.; Zheng, T.; Gao, N.; Li, S.; Kang, J.; Cai, D.; *et al.* Copper Nanowires as Fully Transparent Conductive Electrodes. *Sci. Rep.* **2013**, *3*, 2323.
- (16) Xu, W. H.; Wang, L.; Guo, Z.; Chen, X.; Liu, J.; Huang, X. J. Copper Nanowires as Nanoscale Interconnects: Their Stability, Electrical Transport, and Mechanical Properties. *ACS Nano* **2015**, *9*, 241–250.
- (17) Ravi Kumar, D. V.; Woo, K.; Moon, J. Promising Wet Chemical Strategies to Synthesize Cu Nanowires for Emerging Electronic Applications. *Nanoscale* **2015**, *7*, 17195–17210.
- (18) Jin, M.; He, G.; Zhang, H.; Zeng, J.; Xie, Z.; Xia, Y. Shape-Controlled Synthesis of Copper Nanocrystals in an Aqueous Solution with Glucose as a Reducing Agent and Hexadecylamine as a Capping Agent. *Angew. Chemie - Int. Ed.* **2011**, *50*, 10560–10564.
- (19) Yin, Z.; Lee, C.; Cho, S.; Yoo, J.; Piao, Y.; Kim, Y. S. Facile Synthesis of Oxidation-Resistant Copper Nanowires toward Solution-Processable, Flexible, Foldable, and Free-Standing Electrodes. *Small* **2014**, *10*, 5047–5052.
- (20) Mohl, M.; Pusztai, P.; Kukovec, A.; Konya, Z.; Kukkola, J.; Kordas, K.; Vajtai, R.; Ajayan, P. M. Low-Temperature Large-Scale Synthesis and Electrical Testing of Ultralong Copper Nanowires. *Langmuir* **2010**, *26*, 16496–16502.
- (21) Kevin, M.; Lim, G. Y. R.; Ho, G. W. Facile Control of Copper Nanowire Dimensions via the Maillard Reaction: Using Food Chemistry for Fabricating Large-Scale Transparent Flexible Conductors. *Green Chem.* **2015**, *17*, 1120–1126.
- (22) Kumar, D. V. R.; Kim, I.; Zhong, Z.; Kim, K.; Lee, D. Synthesis of Cu Nanowires : Exploring the Dual Role of Alkyl Amines. *Phys. Chem. Chem. Phys.* **2014**, *16*, 22107–22115.
- (23) Xia, Y.; Xiong, Y.; Lim, B.; Skrabalak, S. E. Shape-Controlled Synthesis of Metal Nanocrystals: Simple Chemistry Meets Complex Physics? *Angew. Chemie - Int. Ed.* **2009**, *48*, 60–103.
- (24) Yang, H. J.; He, S. Y.; Tuan, H. Y. Self-Seeded Growth of Five-Fold Twinned Copper Nanowires: Mechanistic Study, Characterization, and SERS Applications. *Langmuir* **2014**, *30*, 602–610.
- (25) Xiong, Y.; Xia, Y. Shape-Controlled Synthesis of Metal Nanostructures: The Case of Palladium. *Adv. Mater.* **2007**, *19*, 3385–3391.
- (26) Zhang, D.; Wang, R.; Wen, M.; Weng, D.; Cui, X.; Sun, J.; Li, H.; Lu, Y. Synthesis of Ultralong Copper Nanowires for High-Performance Transparent Electrodes. *J. Am. Chem. Soc.* **2012**, *134*, 14283–14286.
- (27) Meng, F.; Jin, S. The Solution Growth of Copper Nanowires and Nanotubes Is Driven by Screw Dislocations. *Nano Lett.* **2012**, *12*, 234–239.
- (28) Sondheimer, E. H. *The Mean Free Path of Electrons in Metals*; 1952; Vol. 1.
- (29) Huang, Q.; Lilley, C. M.; Bode, M.; Divan, R. Surface and Size Effects on the Electrical Properties of Cu Nanowires. *J. Appl. Phys.* **2008**, *104*.
- (30) Huang, Y.-T.; Huang, C.-W.; Chen, J.-Y.; Ting, Y.-H.; Cheng, S.-L.; Liao, C.-N.; Wu, W.-W. Mass Transport Phenomena in Copper Nanowires at High Current Density. *Nano Res.* **2016**, *9*, 1071–1078.
- (31) Huang, Q.; Lilley, C. M.; Divan, R. An *in Situ* Investigation of Electromigration in Cu Nanowires. *Nanotechnology* **2009**, *20*, 75706.
- (32) Durkan, C.; Welland, M. E. Analysis of Failure Mechanisms in Electrically Stressed Gold Nanowires. *Ultramicroscopy* **2000**, *82*, 125–133.
- (33) Yeo, J.; Kim, G.; Hong, S.; Lee, J.; Kwon, J.; Lee, H.; Park, H.; Manoroktul, W.; Lee, M. T.; Lee, B. J.; *et al.* Single Nanowire Resistive Nano-Heater for Highly Localized Thermo-Chemical Reactions: Localized Hierarchical Heterojunction Nanowire Growth. *Small* **2014**, *10*, 5015–5022.
- (34) Durkan, C.; Schneider, M. a; Welland, M. E. Analysis of Failure Mechanisms in Electrically Stressed Au Nanowires Analysis of Failure Mechanisms in Electrically Stressed Au Nanowires. *J. Appl. Phys.* **1999**, *1280*, 1280–1286.